

# Evolution and stability of a magnetic vortex in small cylindrical ferromagnetic particle under applied field

Konstantin Yu. Guslienko\*

Korea Institute for Advanced Study, 207-43 Cheongryangri-dong, Dongdaemun-gu, Seoul 130-012 Korea

Konstantin L. Metlov\*\*

Institute of Physics ASCR, Na Slovance 2, Prague 8, CZ-18221

(November 5, 2018)

The energy of a displaced magnetic vortex in a cylindrical particle made of isotropic ferromagnetic material (magnetic dot) is calculated taking into account the magnetic dipolar and the exchange interactions. Under the simplifying assumption of small dot thickness the closed-form expressions for the dot energy is written in a non-perturbative way as a function of the coordinate of the vortex center. Then, the process of losing the stability of the vortex under the influence of the externally applied magnetic field is considered. The field destabilizing the vortex as well as the field when the vortex energy is equal to the energy of a uniformly magnetized state are calculated and presented as a function of dot geometry. The results (containing no adjustable parameters) are compared to the recent experiment and are in good agreement.

75.75.+a, 75.25.+z, 75.60.-d

*Introduction.* The unusual magnetic properties of sub-micron cylindrical magnetic particles and their periodic two-dimensional arrays drawn much attention because of their possible potential as a magnetic storage as well as an interesting model system for studying of the magnetization reversal<sup>1-4</sup>. The applications of such patterned magnetic films for magnetic information storage (MRAM, for instance) are promising.

In this work the isolated magnetic particles made of isotropic (soft) magnetic material shaped as circular cylinders (referred hereafter as “dots”) are considered. The magnetic properties of the dots are governed by the magnetic dipolar and the exchange interactions. When the external magnetic field is absent, three parameters of the dimension of length define completely the magnetic structure of a dot. These parameters are: the dot radius  $R$ , the dot thickness  $L$  and the exchange length  $L_E = \sqrt{C/M_S^2}$ , where  $C$  is the exchange constant and  $M_S$  is the saturation magnetization of the material. The phase diagram of small  $L/L_E \lesssim 4$ ,  $R/L_E \lesssim 4$  dots in no applied magnetic field showing the range of dot parameters where the magnetic vortex (curl) is the ground state was calculated by Usov and co-workers<sup>5,6</sup>. Vortex states were indeed observed in polycrystalline  $Co^7$  and  $FeNi^{4,8-11}$  cylindrical dots.

So far there is no theory of magnetization reversal of a dot in a vortex state when the magnetic field  $h = H/4\pi M_S$  applied in the direction perpendicular to the cylinder axis. This process taking place via nucleation, displacement and annihilation of a single magnetic vortex<sup>11</sup> is considered in this work. There are three characteristic fields describing this process: the “vortex” nu-

cleation  $h_n$  and annihilation  $h_{an}$  critical fields (for transition to/from the curling state from/to the saturated state) and also the field  $h_{eq}$ , corresponding to the vortex state having the same energy as the uniform one. The size dependent fields of vortex equilibrium  $h_{eq}$  and annihilation  $h_{an}$  are calculated in this paper. The field of vortex nucleation  $h_n$  is determined by the imperfections of the dot shape (and/or material) and was experimentally found to have nearly no correlation to the dot geometry<sup>11</sup>. The field  $h_{eq}$  enters directly the phase diagram in coordinates  $h$ ,  $L/L_E$ ,  $R/L_E$  whose zero field part<sup>6</sup> was already presented.

A realistic description of the non-uniform magnetization distribution in an isolated dot at zero applied field was already considered: first, with the help of guessed trial functions<sup>12</sup> and then using the variational principle<sup>5</sup>. These approaches heavily rely on the cylindrical coordinate system and are hard to generalize for the case when the vortex is deformed by the in-plane magnetic field. Recently, another variational method to construct the magnetization distributions in small exchange-dominated cylinders (not limited to circular ones) was presented<sup>13</sup>. It allows to obtain the structure of a displaced vortex, which is a starting point for the calculations done in this work.

*Equilibrium parameters and stability of displaced vortex.* In a thin ferromagnetic cylinder, with the thickness less or of the order of the exchange length, the magnetization distribution is constant along the thickness and is essentially two-dimensional. In the Cartesian coordinate system with coordinates  $\{X, Y, Z\}$ , chosen in such a way that the axis  $OZ$  is parallel to the cylinder axis, the normalized magnetization vector field  $\vec{m}(\vec{r}) = \vec{M}(\vec{r})/M_S$ ,  $|\vec{m}| = 1$  is independent on the coordinate  $Z$ , so that  $\vec{r} = \{X, Y\}$ . In this case the magnetization distribution corresponding to the minimum of the exchange energy functional

$$E_{ex} = \frac{1}{2}CL \int d^2\vec{r} \sum_{i=X,Y,Z} (\vec{\nabla} m_i(\vec{r}))^2 \quad (1)$$

and having the structure of a displaced magnetic vortex is<sup>13</sup>

$$w(z, \bar{z}) = \begin{cases} \frac{z - a}{c(1 - \bar{a}z)} & |z - a| < c|1 - \bar{a}z| \\ i \frac{(z - a)(1 - a\bar{z})}{|z - a||1 - \bar{a}z|} & |z - a| \geq c|1 - \bar{a}z| \end{cases}, \quad (2)$$

where the components of the magnetization vector are expressed as  $m_x + im_y = 2w/(1 + w\bar{w})$  and  $m_z = (1 - w\bar{w})/(1 + w\bar{w})$  through the complex function  $w(z, \bar{z})$

of the complex variable  $z = X/R + iY/R$ , the horizontal line over a variable denotes the complex conjugation  $\bar{z} = X/R - iY/R$ , the straight brackets stand for the absolute value of a complex number  $|z|^2 = z\bar{z}$ . The expression (2) gives the magnetization distribution minimizing the functional (1) for all values of a scalar parameter  $c$ , related to the radius of the vortex core and a complex parameter  $a = X_C/R + iY_C/R$ , describing the position of the vortex center. The case of  $a = 0$  corresponds to the Usov's vortex solution<sup>5</sup> which satisfies the conditions  $(\vec{m} \cdot \vec{n})_S = 0$  and  $(\partial \vec{m} / \partial \vec{n})_S = 0$  on the side dot boundary. The conformal mapping  $z \Rightarrow (z - a)/(1 - \bar{a}z)$  used<sup>13</sup> to obtain (2) holds the boundary condition  $(\partial \vec{m} / \partial \vec{n})_S = 0$  unchanged, whereas the side magnetic charges  $(\vec{m} \cdot \vec{n})_S$  appear. If the magnetic field is applied along  $Y$  axis it is clear from the symmetry that the vortex will be displaced parallel to the  $X$  axis, which allows to assume that the parameter  $a$  is real. The expression (2) yields correct limiting cases  $a = 0$  (centered vortex) and  $a = 1$  (single-domain or saturated dot) and is applicable at small enough  $R$  and  $L$ . The example distribution at an intermediate value of  $a$  is given in Fig. 1. To find particular values of the parameters  $a$  and  $c$  corresponding to the given dot geometry, material and applied magnetic field it is necessary to include into consideration the magnetostatic and Zeeman energies.

The magnetostatic energy has two surface (on the dot faces and sides) and a negligible (for small dot thickness) volume contributions. To simplify the further consideration we shall assume that the dot thickness is small enough to neglect the volume magnetostatic contribution.

In the further calculations two polar coordinate systems with the same notation for coordinates  $r, \phi$  will be used. One of the coordinate systems will be centered in the dot center and have the dimensionless polar radius  $\rho = r/R$ . The other coordinate system centered at the vortex core center is also polar, because the vortex core (the region of the dot with non-zero  $m_z$ ) has exactly the circular boundary for all values of  $a$ . The center of the vortex core (note the difference with the vortex center where  $m_z = 1$ ) is situated at the coordinates  $X_V = a(1 - c^2)/(1 - a^2c^2)$ ,  $Y_V = 0$  for real  $a$ , and its radius  $R_V = c(1 - a^2)/(1 - a^2c^2)$ . The dimensionless polar radius for the coordinate system centered at the vortex core is  $\rho = r/R_V$ .

The density of magnetic charges produced by the distribution (2) on the faces of the dot in the polar coordinate system centered at the vortex core is

$$m_z = \sigma(\rho, \phi) = \cos \delta \frac{1 - \rho^2}{1 + \rho^2 - 2\rho \sin \delta \cos \phi}, \quad (3)$$

with  $\delta = 2 \arctan(ac)$ . The magnetostatic energy of these charges normalized to  $4\pi M_S^2 V$  ( $V = L\pi R^2$  is the dot volume, all energies further in the text will be given in this normalization) is

$$e_{MS}^{\text{face}} = \frac{E_{MS}^{\text{face}}}{4\pi M_S^2 V} = \frac{R_V^3}{LR^2} (G(0) - G(L/R_V)), \quad (4)$$

where

$$G(x) = \int \frac{\sigma(\rho_1, \phi_1)\sigma(\rho_2, \phi_2)\rho_1 d\rho_1 \rho_2 d\rho_2 d\phi_1 d\phi_2}{(2\pi)^2 \sqrt{x^2 + \rho_1^2 + \rho_2^2 - 2\rho_1\rho_2 \cos(\phi_1 - \phi_2)}}, \quad (5)$$

the integration runs from 0 to 1 in  $\rho_1, \rho_2$  and from 0 to  $2\pi$  in  $\phi_1, \phi_2$ . Assuming that the parameter  $ac$  is small (which is justified by our numerical calculations, also see the caption to Fig. 1) the last expression in zero-th order in  $ac$  is

$$e_{MS}^{\text{face}} = \frac{c^3(1 - a^2)^3}{g} \left( G_U(0) - G_U\left(\frac{g}{c(1 - a^2)}\right) \right) \quad (6)$$

where  $G_U(x) = G(x, \delta \rightarrow 0)$  is the magnetostatic function of non-displaced vortex core<sup>5</sup> and  $g = L/R$ . While this expression is approximate it captures the details of the exact one (4) well, and has error not more than 1% as we have checked numerically.

The surface magnetic charges on the sides of the dot are

$$(\vec{m} \vec{n})_S = \sigma(\phi) = 2a \sin \phi \frac{a \cos \phi - 1}{1 + a^2 - 2a \cos \phi}, \quad (7)$$

which is written in the cylindrical coordinate system  $r, \phi$  centered at the dot center. The energy of these charges can be expressed as

$$e_{MS}^{\text{side}} = \int \frac{\sigma(\phi_1)\sigma(\phi_2) dz_1 dz_2 d\phi_1 d\phi_2}{2g(2\pi)^2 \sqrt{2(1 - \cos(\phi_1 - \phi_2)) + (z_1 - z_2)^2}}, \quad (8)$$

where the integration runs from 0 to  $g$  in  $z_1, z_2$  and from 0 to  $2\pi$  in  $\phi_1, \phi_2$ . The last expression can be simplified using the summation theorem for the Bessel's functions into

$$e_{MS}^{\text{side}} = \frac{1}{2} \left[ a^2(a^2 - 2)^2 I_1(g) + (1 - a^2)^2 \sum_{\mu=1}^{\infty} a^{2\mu} I_{\mu}(g) \right] \quad (9)$$

$$I_{\mu}(g) = \int_0^{\infty} \frac{dk}{k} \left( 1 - \frac{1 - \exp(-kg)}{kg} \right) J_{\mu}^2(k), \quad (10)$$

where  $J_{\mu}(x)$  is the Bessel's function of the first kind and order  $\mu$ . Minimizing the total energy we have kept only one term in the above series, which was sufficient to have the error less than 3%.

The total magnetization of the dot (having only one non-zero component along  $Y$  axis), which enters the Zeeman energy is

$$\langle m_y \rangle = \int \frac{((1 + a^2)\rho \cos \phi - a(1 + \rho^2))\rho d\rho d\phi}{\sqrt{a^2 + \rho^2 - 2a\rho \cos \phi} \sqrt{1 + a^2\rho^2 - 2a\rho \cos \phi}}, \quad (11)$$

where the integration from 0 to 1 in  $\rho$  and from 0 to  $2\pi$  in  $\phi$  is performed in the coordinate system centered on the dot. This integral can be approximated by  $\langle m_y \rangle = a(15a^4 + 34a^2 - 193)/144$  with the error less than 1% according to our numerical calculations.

The exchange energy can be evaluated using its expression<sup>13</sup> directly through the function  $w(z, \bar{z})$ , or, alternatively, using (1) as

$$e_{\text{EX}} = \frac{1}{4\pi} \left( \frac{L_E}{R} \right)^2 (2 - \log(c)), \quad (12)$$

which is independent on  $a$ .

The total energy density of the particle is  $e = e_{\text{ex}} + e_{MS}^{\text{face}} + e_{MS}^{\text{side}} - h\langle m_y \rangle$  and should be minimized with respect to the parameters  $a$  and  $c$ . These parameters are coupled through the  $e_{MS}^{\text{face}}$  term which depends on both of them. However, if we use  $q = c(1 - a^2)/g$  instead of  $c$  the parameters  $a$  and  $q$  become decoupled and the energy can be minimized with respect to each independently.

The only terms depending on  $q$  are  $e_{\text{EX}} + e_{MS}^{\text{face}} = \lambda^2 g^2 (2 - \log qq) + q^3 g^2 Q(1/q) + \text{const}$ , where  $Q(x) = G_U(0) - G_U(x)$ ,  $\lambda = L_E/(L\sqrt{4\pi})$ . The equilibrium value of  $q$ , then, satisfies the following equation

$$q \frac{d}{dq} [q^3 Q(1/q)] = \lambda^2, \quad (13)$$

which is exactly the equation<sup>5,6</sup> for the equilibrium radius of the vortex core at zero field.

The rest of terms in the total energy  $e_1(a, h) = e_{MS}^{\text{side}} - h\langle m_y \rangle + \lambda^2 g^2 \log(1 - a^2)$  depend only on  $a$ , the last term comes from the exchange energy after changing the independent variable from  $c$  to  $q$ .

The vortex loses its stability when at a certain value of the external field  $h = h_{\text{an}}$  the energy minimum it is in turns to a saddle point or a maximum. This leads to the following system of equations for  $a_{\text{an}}, h_{\text{an}}$ :

$$\begin{cases} \partial e_1(a_{\text{an}}, h_{\text{an}})/\partial a_{\text{an}} = 0 \\ \partial^2 e_1(a_{\text{an}}, h_{\text{an}})/\partial a_{\text{an}}^2 = 0. \end{cases} \quad (14)$$

These equations were solved numerically for  $L_E/L = 18 \text{ nm}/15 \text{ nm}$  (corresponding to the experiment<sup>11</sup>) and the resulting dependence of the vortex annihilation field  $h_{\text{an}}$  on the reduced dot radius  $1/g = R/L$  is shown in Fig. 2. The resulting  $h_{\text{an}}(1/g)$  curve agrees well with the experimental points<sup>11</sup>.

The field  $h_{\text{eq}}$  when the energy of the displaced vortex in the external magnetic field is equal to the energy of the uniformly magnetized state was determined from the equations:

$$\begin{cases} \partial e_1(a_{\text{eq}}, h_{\text{eq}})/\partial a_{\text{eq}} = 0 \\ e_1(a_{\text{eq}}, h_{\text{eq}}) = e_{MS}^{\text{side}}(a \rightarrow 1) - h_{\text{eq}}, \end{cases} \quad (15)$$

and also plotted in Fig. 2. This expression takes into account the fact that the exchange and the face magnetostatic energies are equal to zero for the single-domain (saturated in-plane) dot.

*Discussion.* The calculations of the annihilation field explain reasonably the experiment over a wide range of  $1/g$ . The differences between the measured and calculated  $h_{\text{an}}$  curves at small  $R/L < 10$  can be the result of increasing role of thermal fluctuations in small particles. The peak on the calculated dependencies of both  $h_{\text{an}}$  and  $h_{\text{eq}}$  on  $R$  (see Fig. 2) due to their decrease with the cylinder radius at small  $R$  is not present in the experimental data<sup>11</sup> and needs an explanation.

It can be explained as the result of inherent (not requiring the applied field) instability of vortex in the cylinders of small radius. There are two kinds of forces acting on the vortex in a cylinder, the stabilizing (due to the energy terms increasing as the vortex comes off the dot center)

and destabilizing ones. In the case considered in this paper the main stabilizing force is produced by the energy of magnetic charges on the cylinder side. The rate of the increase of this energy term (9) with  $a$  (the actual force) decreases with the dot radius  $R$  at a fixed  $L$ . This decrease is related to the decrease in the possible amount of magnetic charges forming (the area of side decreases with  $R$ ) and also to the decreasing distance between the positive and negative ones, whose negative interaction energy strengthens as a result.

The destabilizing force is due to the energy of the magnetic charges on the cylinder faces (4), which is positive for the centered vortex and is zero when the vortex is completely out of the cylinder. This force is independent on the dot radius as long as the vortex core fits completely within the particle.

Therefore, as the radius of the cylinder decreases there is a point (called the stability radius  $R_S$ ) where the destabilizing force starts to outweigh the stabilizing one and the vortex becomes unstable in such a cylinder. If the cylinder radius is smaller than  $R_S$  *no magnetic field is required* to destabilize the vortex and  $h_{\text{an}} = 0$ . This means that the field  $h_{\text{an}}$  decreases at small cylinder radii to become zero at  $R = R_S$ .

The similar decrease of  $h_{\text{eq}}$  happens because the smaller is the cylinder the smaller is the energy of the uniformly magnetized state in it and it is closer to the energy of the cylinder with a vortex. Until, at the so-called single domain radius  $R_C$  these energies become equal with no applied field. This means at small radii  $h_{\text{eq}}$  also decreases with the radius until it is exactly zero at  $R = R_C$ .

The values of both  $R_S$  and  $R_C$  have sense only when they are larger than the vortex core radius  $R_V$ . This is not the case for the cylinder thickness  $L/L_E = 15/18$  shown in Fig. 2, where  $R_S < R_V$ ). Our calculations show that at smaller dot thicknesses the case when  $R_S, R_C > R_V$  can be realized and  $h_{\text{an}}, h_{\text{eq}}$  curves start from zero at small radii.

As we have mentioned in the introduction, the dependence of  $R_C/L_E$  on  $L/L_E$  was already reported in literature<sup>6</sup>, its calculation does not require a model of displaced vortex. The coincidence of the cylinder radius at which  $h_{\text{eq}}$  turns to zero with  $R_C$  was one of the checks we did to verify the results.

The approximations we performed were focused on calculating the dot energy at arbitrarily large vortex displacements, that is, not to perform a perturbative expansion limiting us to a particular range of displacements. However, for the calculation of  $R_S$  corresponding to the vortex displacement mode given by Eq. (2) the expansion at  $a = 0$  up to second order is enough. The approximations done here, especially Eq. (6), are, strictly speaking, not valid up to the second order in  $a$  at  $a = 0$ . Therefore, the stability radius resulting from this calculation should be taken with caution. The mentioned expansion is easy to perform and we plan to present the precise estimate of  $R_S$  for the mode (2) in one of our forthcoming papers.

Some correlation of the vortex annihilation field with the dot average in-plane demagnetization factor in saturated state was already noted<sup>7</sup>. That can be explained as

follows. The vortex shift  $a$  in the external magnetic field is determined by competition of the side magnetostatic and Zeeman energies. The main contribution in Eq. (9) to the magnetostatic energy from the dot boundary is proportional to  $I_1(g)$  being exactly the single-domain dot in-plane average demagnetization factor<sup>14</sup>. But this is correct only for large enough dot radius (considerably above  $R_S, R_C$ ) when the face magnetostatic energy and exchange energy can be neglected.

*Conclusions.* In summary, the size-dependent vortex equilibrium and annihilation fields have been studied theoretically for circular cylindrical magnetic dots. Simple analytical approximation suggested for the dot magnetization distribution allowed us to consider the transition from the vortex to single-domain dot magnetization state under applied magnetic field. The calculation results agree well with the experimental data within the limit of weak inter-dot coupling. Further studies of static and dynamic properties of magnetization in isolated and magnetostatically coupled dots are in progress.

The support by Korea Institute for Advanced Study is gratefully acknowledged. The work was supported in part by the Grant Agency of the Czech Republic under projects 202/99/P052 and 101/99/1662.

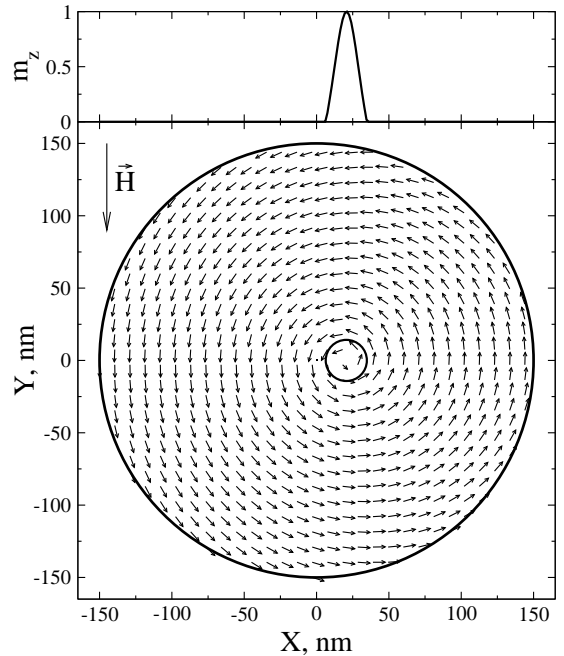


FIG. 1. The magnetization distribution (2) with the equilibrium values  $a \approx 0.14$  and  $c \approx 0.092$  corresponding to a permalloy ( $L_E = 18 \text{ nm}$ ) cylinder with  $R = 150 \text{ nm}$ ,  $L = 15 \text{ nm}$  in the magnetic field  $h = H/(4\pi M_S) = -0.025$  applied parallel to the cylinder  $OY$  axis. The out-of-plane magnetization component on the line  $Y = 0$  is shown on the upper plot.

\* On leave from the Institute for Magnetism, 36 Vernadsky str., 03252 Kiev, Ukraine.

\*\* Corresponding author. Electronic address: metlov@fzu.cz

<sup>1</sup> C. Miramond *et al.*, J. Magn. Magn. Mat. **165**, 500 (1997).

<sup>2</sup> E. F. Wassermann *et al.*, J. Appl. Phys. **83**, 1754 (1998).

<sup>3</sup> R. P. Cowburn, J. Phys. D: Appl. Phys. **33**, R1 (2000).

<sup>4</sup> T. Pokhil, D. Song, and J. Nowak, J. Appl. Phys. **87**, 6319 (2000).

<sup>5</sup> N. A. Usov and S. E. Peschany, J. Magn. Magn. Mat. **118**, L290 (1993).

<sup>6</sup> N. A. Usov and S. E. Peschany, Fiz. Met. Metal **12**, 13 (1994), (in russian).

<sup>7</sup> A. Fernandez and C. J. Cerjan, J. Appl. Phys. **87**, 1395 (2000).

<sup>8</sup> R. P. Cowburn *et al.*, Phys. Rev. Lett. **83**, 1042 (1999).

<sup>9</sup> T. Shinjo *et al.*, Science **289**, 930 (2000).

<sup>10</sup> J. Raabe *et al.*, J. Appl. Phys. **88**, 4437 (2000).

<sup>11</sup> M. Schneider, H. Hoffmann, and J. Zweck, Appl. Phys. Lett. **77**, 2909 (2000).

<sup>12</sup> A. Aharoni, J. Appl. Phys. **68**, 2892 (1990).

<sup>13</sup> K. L. Metlov, arXiv:cond-mat/0012146 (unpublished).

<sup>14</sup> K. Y. Guslienko, S.-B. Choe, and S.-C. Shin, Appl. Phys. Lett. **76**, 3609 (2000).

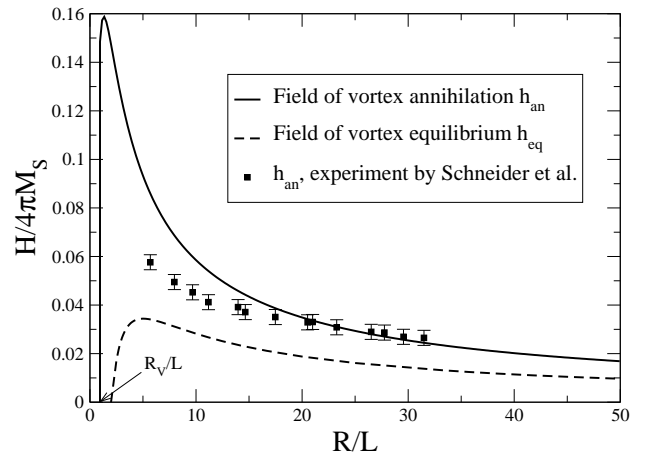


FIG. 2. Characteristic fields of the permalloy  $L_E = 18 \text{ nm}$  dots of the thickness  $L = 15 \text{ nm}$  as a function of their radius. The experimental points are taken from the literature<sup>11</sup>.